

EVALUATION OF SINTERED CARBIDES MICROSTRUCTURE THROUGH AUTOMATIC IMAGE ANALYSIS

Janusz RICHTER, Jan CWAJNA, Janusz SZALA

Silesian University of Technology, Department of Materials Science
ul. Krasińskiego 8, PL-40-019 Katowice, Poland

ABSTRACT

Stereological parameters characterizing structural components of WC-Co type sintered carbides of various (fine, coarse and super-coarse) structure were assessed. Empirical equations relating structure and properties (coercive force) of these materials were verified. The obtained result, enabled recommendation of quantitative metallography and automatic image analysis as method of accurate assessment of sintered carbides microstructure.

Key words: image analysis, sintered carbides, stereology

INTRODUCTION

Sintered carbides are known and applied since 1923 when Shröter (Fishmeister, 1981) produced sintered material from WC and Co. Numerous studies devoted improvement of chemical composition and technology of these materials led to their broad (and still increasing) development. Stability of sintered carbides' properties is of special importance since tools made of them are predominantly employed in automatic machine production lines which shutdown frequency depends on the weakest component durability. In this respect evaluation of quality at each stage of sintered carbides production becomes significant factor of these materials development. Because of its simplicity and nondestructive character, measurements of a coercive force of sintered carbides inserts and other products is widely applied in industrial quality inspection. Numerous empirical relations between this magnetic property and main structure features (carbide particles size, binding phase fraction, mean free path of cobalt binder) determining service properties, are to be found in the literature. The aim of this paper is to verify these structure-property relations using a quantitative metallography, stereology and image analysis methods.

EXPERIMENTAL

Main goals of the study were: working out methods of sintered carbides' investigations with scanning electron microscopy, stereology and image analysis as well as recommendation of

parameters adequately describing microstructure of sintered carbides. Hence the following research programme was established:

- measurements of sintered carbides' basic properties,
- preparation of microsections to be observed with field emission (FE) SEM,
- selection of FE SEM working conditions,
- working out morphological operations enabling automatic image analysis,
- verification of literature data concerning structure-property empirical relations.

Four grades of WC-Co type carbides of various grain size and similar content of binding phase were chosen:

- Baildon H30 (fine-grained),
- Baildon B23 (coarse-grained),
- Baildon B23G (super coarse-grained),
- Boart (super coarse-grained).

Coercive force H_C of sintered carbides is related to mean grain diameter \bar{d} and mean free path of cobalt binder $\bar{\lambda}$ (Porat et al., 1987):

$$V_V(\text{Co}) = \frac{X_{\text{Co}}}{8.9} \cdot \frac{\rho_{\text{sp}}}{100} \quad (1)$$

$$\bar{d} = 0.3 \left(\frac{80}{H_C} \right)^{0.57 [V_V(\text{Co})]^{-\frac{1}{3}}} \quad [\mu\text{m}] \quad (2)$$

$$\bar{\lambda} = \bar{d} \frac{V_V(\text{Co})}{1 - V_V(\text{Co})} \quad [\mu\text{m}] \quad (3)$$

- $V_V(\text{Co})$ - volume fraction of cobalt
 X_{Co} - weight percentage of cobalt
 ρ_{sp} - specimen's density

Therefore magnetic measurements of the specimens were performed with Förster 1.093 measuring device used in current quality control of sintered carbides (Zok, 1995). Specimens' description, cobalt contents, measured densities and coercive forces as well as stereological parameters calculated according to formulae 1-3 are collected in Table 1.

Table 1. Measurements (X_{Co} , ρ_{sp} , H_C) and calculations ($V_V(\text{Co})$, \bar{d} , $\bar{\lambda}$) results.

Grade	X_{Co} [wt. %]	ρ_{sp} [g/cm ³]	H_C [kA/m]	$V_V(\text{Co})$ [%]	\bar{d} [μm]	$\bar{\lambda}$ [μm]
H30	9.0	14.62	13.2	14.8	2.09	0.36
B23	9.5	14.53	7.9	15.6	3.48	0.64
B23G	9.5	14.50	4.0	15.6	7.15	1.32
Boart	9.5	14.56	4.1	15.6	6.97	1.28

After having tested several methods of structure revealing, etching with Murakami reagent for 3 minutes, rinsing with destilated water, drying with alcohol and subsequent etching with Nital (4% ethyl solution of HNO_3) for 2 minutes assured images quality required for automatic image analysis. The SE and BSE images were obtained using Hitachi S-4200 FE SEM. The BSE images proved to be of better contrast than SE ones (Fig. 1), hence they were given further image processing. On each specimen 10 randomly chosen fields were analysed. It was assumed that one measuring field should comprise from 30 up to 50 grains, consequently the following magnifications were employed: H30 - 7000X, B23 - 4500X, B23G - 1500X, Boart - 1000X. Observations at various magnifications were performed with constant accelerating voltage of 20 kV.

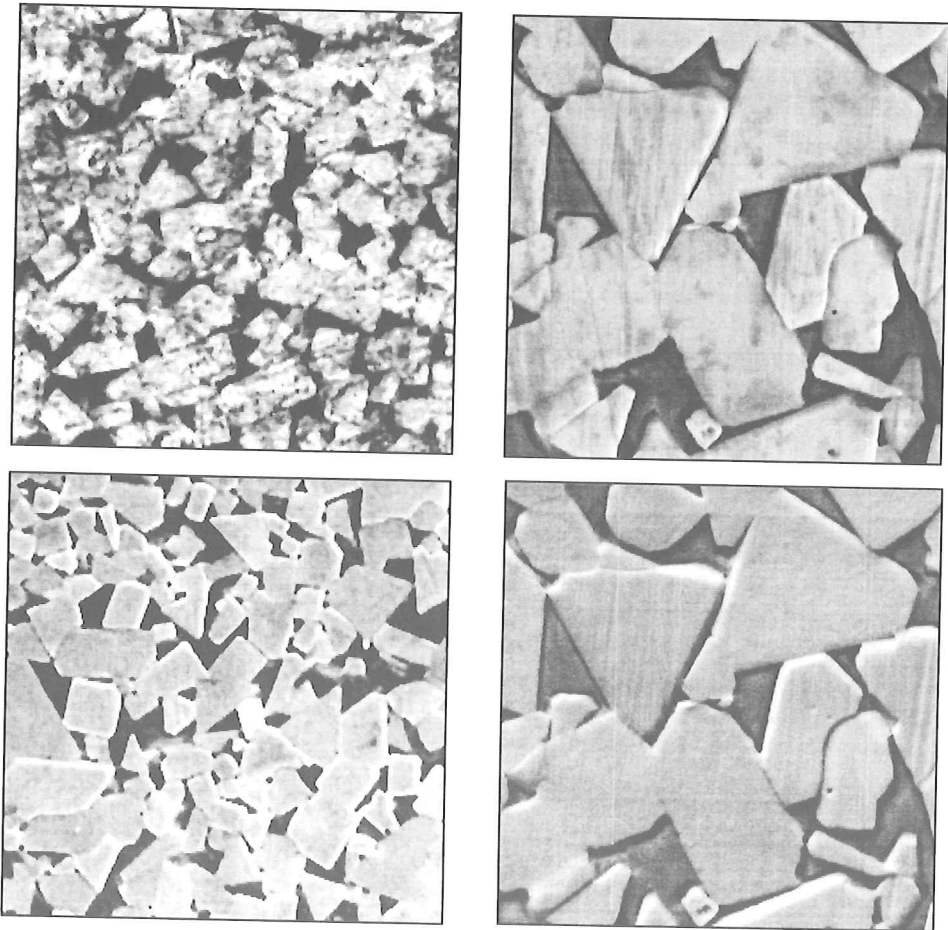


Fig. 1. Comparison of SE (top row) and BSE (bottom row) images of B23 (left) and B23G (right) grades

Images of the structures were transferred to Morphopericolor automatic image analyser in a numerical form. On having tried available morphological operations, their optimal sequence was worked out, which enabled automatic detection of the relevant structural components (Fig. 2, 3). Segmentation is a crucial operation in sintered carbides' image analysis (Gauthier et al.1994). First stage of segmentation (Fig. 2c) was performed using standard procedure available in Morphopericolor automatic image analyser. Since this method yields some excessive boundaries, additional criterion enabling identification and removal of these lines was indispensable. Therefore 'conditional segmentation' (Szala, 1992) was employed to enhance quality of the final binary image (Fig. 2d)

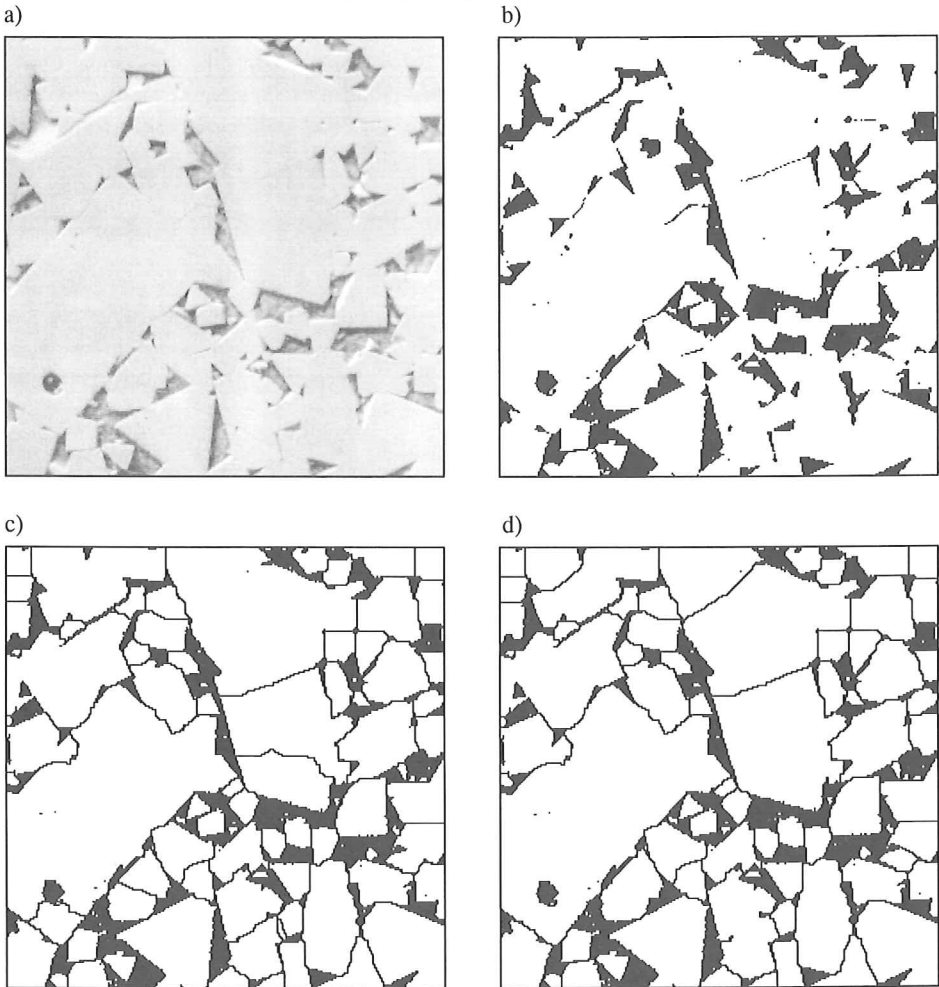


Fig. 2. Application of morphological operations in image processing (Boart specimen): initial numerical image (a), detected binary image (b), image (b) after segmentation (c), and final image of cobalt path (d).

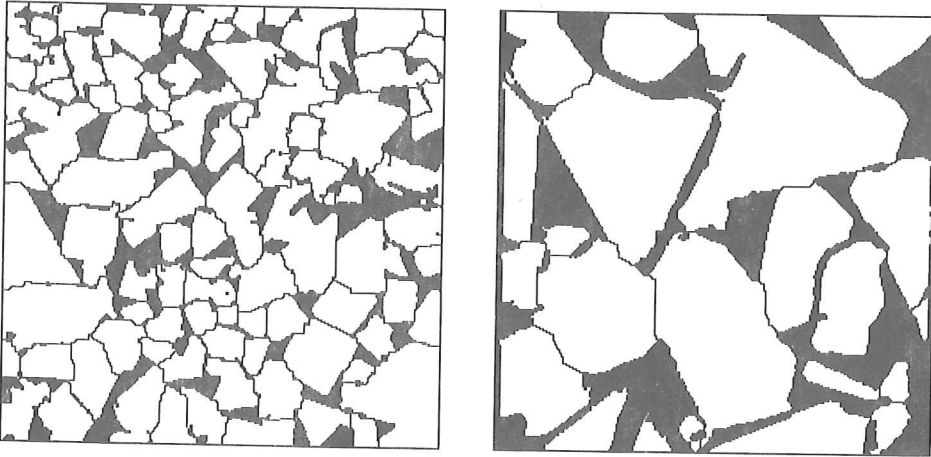


Fig. 3. Detected carbide particles (white areas) of B23 (left) and B23G (right) grades.

MORPHO software (Szala, 1992) were used to verify main stereological parameters (binding phase volume fraction, mean grain size, cobalt free path mean width), the results together with these calculated from equations 1-3 are collected in Table 2.

Table 2. Comparison of calculated and measured parameters

Grade	$V_v(\text{Co})$ [%]			\bar{d} [μm]			$\bar{\lambda}$ [μm]		
	cal.	meas.	RE	cal.	meas.	RE	cal.	meas.	RE
H30	14.80	12.26	17.2	2.09	1.91	8.6	0.36	0.42	16.7
B23	15.60	21.98	40.9	3.48	2.55	26.7	0.69	0.82	28.1
B23G	15.60	19.21	23.1	7.15	10.06	40.7	1.32	2.94	122.7
Boart	15.60	16.28	4.4	6.97	7.01	0.6	1.28	1.94	51.6

Note: cal. - calculated, meas. - measured, RE - relative error [%]

It is to be seen that except values of $V_v(\text{Co})$ and \bar{d} obtained for the Boart specimens, differences between calculated and measured stereological parameters are very large. These findings testify that assessment of microstructure features of sintered carbides using empirical relations containing coercive force yields inaccurate results. Therefore thorough quantitative assessment of the investigated hard metals' structural components were performed.

Carbide particles size were characterized with statistical distribution (commonly applied for evaluation of dispersed phase particles) and geometrical one (Fig. 4). The statistical distribution indicates that B23 and H30 are of similar carbide particles size. In B23G grade values of area of carbide particles plane section fall in 8-50 μm^2 range whereas in case of Boart specimen this interval amounts 20-315 μm^2 . The geometrical distribution much better differentiates individual grades in respect of carbide particles size. Area fraction

occupied by fine grades is the highest for B23 and H30 samples. The characteristic feature of Boart grade is the largest, among the examined samples, area fraction of the coarse carbides.

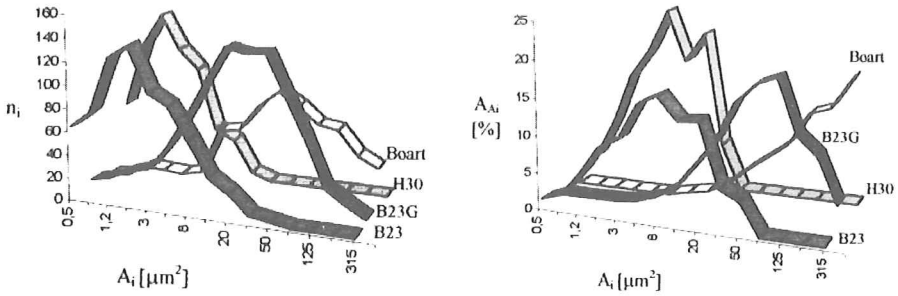


Fig. 4. Statistical (left) and geometrical (right) distributions of carbide particles size.

Comparison of parameters characterizing mean value and variance of carbides size in both distributions (Table 3) leads to conclusion that weighted mean value of geometrical distribution \bar{A}_G is much more sensitive parameter than arithmetic mean in statistical distribution.

Table 3. Parameters obtained with MORPHO software.

Parameter (_s)-statistical (_G)-geometrical	Sintered carbide grade			
	H30	B23	B23G	Boart
Carbide particles size: A-area of plane section, ν -coefficient of variation				
$\bar{A}_S[\mu\text{m}^2]$	2.89	5.13	38.68	88.53
$\nu(A)_S[\%]$	93.62	129.86	126.42	115.82
$\bar{A}_G[\mu\text{m}^2]$	5.43	13.77	100.52	207.28
$\nu(A)_G[\%]$	76.20	94.24	92.07	66.69
Carbide particles shape: ξ -shape factor ($4\pi A/\text{perimeter}^2$)				
$\bar{\xi}_S$	0.39	0.42	0.45	0.43
$\nu(\xi)_S[\%]$	34.96	32.69	29.30	33.78
$\bar{\xi}_G$	0.37	0.36	0.39	0.35
$\nu(\xi)_G[\%]$	39.04	39.84	39.83	46.45

Table 3 (cont.)

Cobalt path characteristics: l-intercept length				
Parameter	H30	B23	B23G	Boart
$\bar{A}_s[\mu\text{m}^2]$	0.43	2.00	14.83	23.90
$\nu(A)_s[\%]$	166.59	179.70	215.57	177.57
$\bar{A}_G[\mu\text{m}^2]$	1.63	8.47	83.75	99.25
$\nu(A)_G[\%]$	168.14	100.39	105.07	91.35
$\bar{l}_s[\mu\text{m}^2]$	0.42	0.82	2.94	1.94
$\nu(l)_s[\%]$	73.43	80.47	89.38	80.10
$\bar{l}_G[\mu\text{m}^2]$	0.65	1.35	3.49	4.83
$\nu(l)_G[\%]$	67.92	67.92	78.82	61.98

The examined specimens differ also in respect of carbide grains size inhomogeneity. The most inhomogeneous grains were found in B23 hard metal and the most homogeneous in Boart one, taking coefficient of variation in geometrical distribution as an inhomogeneity measure.

Carbide particles shape was characterized with statistical and geometrical distributions of shape factor. Both distributions testified that the grains in the examined specimens were of similar shape. The best characteristic of grain shape provided curve of shape factor versus area of carbide plane section (Fig. 5)

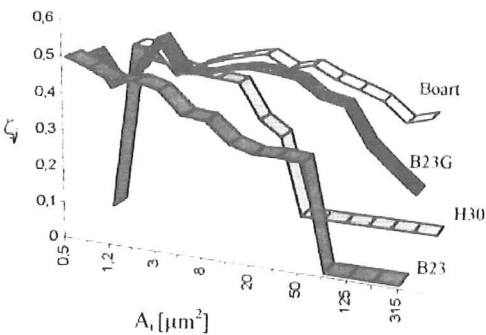


Fig. 5. Characteristic of carbide particles shape.

Areas occupied by cobalt binder were assessed through two distributions - of plane section area and of chord length determined with intercept method. Parameters of these distributions (Table 3) show considerable differentiation of both mean size of cobalt binder islands and their size inhomogeneity. The finest islands occurred in H30 grade, then in B23, B23G and Boart specimens. The highest inhomogeneity of cobalt binder areas was found in the fine grained hard

metal, the others exhibited similar values of parameters characterizing by geometrical distribution the size of cobalt path. On the basis of geometrical distribution of cobalt thickness and its variation coefficient it is to be noticed that in B23G grade the cobalt path is of the most inhomogeneous thickness whereas Boart specimens were of the most homogeneous size of the binding phase.

CONCLUSIONS

On the basis of the results obtained in this study it can be concluded that:

1. The optimal preparation of the sintered carbides specimens to be analysed using FE SEM and automatic image analysis comprises two-stage etching with Murakami and Nital reagents and recording of the BSE images using 20kV accelerating voltage.
2. For individual specimens, magnifications should be chosen so as to each of 10 measuring fields contained 30 up to 50 carbides (they proved to vary between 1000 and 7000X).
3. The worked out image analysis method enables obtaining images suitable for fully automatic measurements of microstructural components' stereological parameters of coarse and super coarse-grained specimens; fine-grained specimens required some minor manual corrections of the images.
4. The method of microstructure evaluation based on coercive force measurements and empirical formulae, commonly applied in sintered carbides quality inspection, proved to be of low accuracy. Therefore it is advisable to introduce the presented quantitative metallography method to quality control of sintered carbides.
5. The following set of stereological parameters may be recommended for evaluation of industrial grades of sintered carbides:
 - a) $V_V(\text{WC})$ - volume fraction of the carbide particles and $V_V(\text{Co})$ - volume fraction of the binding phase,
 - b) geometrical distribution of carbides grain size $A_{A_i}=f(A_i)$ and its \bar{A}_G and $\nu(A)_G$ parameters,
 - c) characterization of carbide particles shape through $\zeta_i=f(A_i)$ distribution,
 - d) geometrical distribution of cobalt path plane section $A_{A_i}=f(A_i)$ together with its parameters \bar{A}_G and $\nu(A)_G$, which show degree of cobalt path contiguity, geometrical distribution of cobalt path thickness $L_{L_i}=f(l_i)$ and its parameters \bar{l}_G and $\nu(l)_G$.

ACKNOWLEDGEMENT

The financial support from the Committee of Scientific Research, grant No 7T08A 02509 is gratefully acknowledged. We are also indebt to Jan Krajzel MSc from Steel Plant BAILDON for valuable discussion and specimen material.

REFERENCES

- Fishmeister H.F.: Development and present state of sintered carbides technology. Int.Conf. for Sintered Carbides. Jackson Lake Lodge, Moran, Wyoming, USA, 23-28 August, 1981.
- Gauthier G., Quenec'h J.L., Coster M., Chermant J.L.: Segmentation of grains boundaries in WC-Co cermets. 6 ECS Praha, Czech Republic, 7-10 September, 1993, Acta Stereol. 1994, 13, 209-214.
- Porat P., Malek J.: Binder mean-free-path determination in cemented carbides by coercive force and material composition, Mater. Sc. Eng., 1988, A 105/106: 289-292.
- Szala J.: MORPHO-software, Silesian University of Technology, 1992 (unpublished).
- Zok S.: The effect of microstructure upon sintered carbides' physical properties. MSc thesis. Silesian Technical University. Katowice 1995.